# Fracture Behavior of W-Ni-Fe Heavy Alloys

K. S. CHURN and R. M. GERMAN

Heavy alloys were liquid phase sintered from compacts of mixed W, Ni, and Fe powders. The alloy compositions ranged from 93 to 97 wt pct W, with the Ni:Fe ratio maintained at 7:3. Sintering was performed under hydrogen in the 1465 to 1485 °C temperature range, giving full density within the first 15 minutes. The room temperature strength and ductility showed major degradation with sintering times in excess of two hours. Tensile tests and bend tests have been performed to isolate the fracture mode and the property determining features. Initial cracking occurs at the tungsten-tungsten grain boundaries and in the tungsten grains. These latter cracks propagate through the structure to give eventual failure. The ductility to failure is shown to be governed by the strength of the tungsten-matrix interface. The maximum elongation depends on the contiguity, which in turn is set by the alloy composition.

## I. INTRODUCTION

THE heavy alloys constitute several tungsten based two phase composites which rely on various Cu, Ni, or Fe additions to form a ductile matrix. These alloys are used in diverse applications ranging from radiation shields to counter balances. Recent strong attention has been focused on the mechanical properties of these alloys and the observed sensitivity in ductility. There are two general goals in current research with heavy alloys: (1) improve the overall properties (higher strength, ductility, and toughness), and (2) isolate and avoid the causes of embrittlement.

As the tungsten content increases, the density of the alloy increases. Additionally, the material decreases in ductility and has a greater sensitivity to sources of embrittlement. There are several variables which influence the mechanical properties of heavy alloys. This list includes the impurities, sintering conditions, post-sintering treatments, and the testing conditions. Recent findings have been somewhat contradictory in that the causes of embrittlement have been given as intermetallic phase formation, impurity segregation, hydrogen embrittlement, shrinkage pore formation, and a varying ductile-brittle transition temperature.

Edmonds and Jones[1] found intermetallic phase formation at the matrix tungsten interface in a 90W-5Ni-5Fe alloy and gave this as a cause for embrittlement. This has also been suggested as the cause of embrittlement in slow cooled alloys with a Ni:Fe ratio of 7:3.[2,3] However, Henig, *et al.*[4] claim no detrimental effect from this intermetallic. Other investigators[5] have been unable to confirm the existence of this phase in embrittled material with a 1:1 ratio of Ni:Fe. Several reports[1,6-8] have shown a strong impurity influence, wherein the elements such as P and S segregate to the tungsten-matrix interface during slow cooling from elevated temperatures (over approximately 800 °C). Yoon *et al.*[9] and others[10,11] found strength and ductility degraded by heating in a hydrogen atmosphere. The effect of hydrogen is to weaken the tungsten-matrix interface. Kang *et al.*[12] have shown mechanical property decrements due to rapid cooling from the sintering temperature. The formation of matrix phase solidification porosity with rapid cooling is quite detrimental to the properties; Churn and Yoon[13] have given a clear demonstration of the porosity effect.

The fracture behavior of the tungsten heavy metals has been explored by several investigators. Krock and Shepard[14] proposed that crack initiation was at the grain surface, while crack growth is governed by the matrix phase. Several other investigations[13,15-20] have observed preferential cracking at the tungsten-tungsten grain boundaries with cleavage failure of the tungsten grains. It has been demonstrated that embrittled material exhibits decohesion at the tungsten-matrix interface. The fracture studies in the past have been unclear as to the exact failure mechanism. There are obvious differences in the fracture surface, but the sequence of steps during failure contributing to the differences has not been isolated. Furthermore, most of the research has focused on determining processing effects on properties, with secondary attention to the mechanism. In this investigation we have examined the mechanisms of crack propagation. The variations in ductile *vs* brittle failure were created by adjustment of the sintering time. Furthermore, microstructurally limited ductility has been assessed by the contiguity. This study demonstrates the microscopic mechanism of failure in tungsten heavy alloys and suggests that attention to the tungsten-matrix interface is appropriate for property optimization.

## II. EXPERIMENTAL APPROACH

Tensile specimens of various tungsten contents from 93 to 97 wt pct W were prepared by liquid phase sintering of blended, elemental powders. The Ni to Fe ratio was maintained at 7:3, in accord with the prior optimization studies.[19,21] The characteristics of the three powders are given in Table I. The preweighed powders were ball milled for 48 hours. For green strength, 1 pct paraffin wax dissolved in benzene was added to the milled powder. Compacts were prepared using the standard MPIF tensile geometry at pressures of 210 MPa. The tensile bars were presintered at 920 °C for three hours in hydrogen to remove the binder. Subsequently, the bars were sintered at temperatures between 1465 and 1485 °C (depending on the tungsten content) for times up to 15 hours in a dry hydrogen atmosphere. Temperature was controlled to within ±5 °C of the setpoint, with approximate heating and cooling rates of 150 °C per minute.

K. S. CHURN, formerly a Postdoctoral Fellow at RPI under a fellowship from the Korea Science and Engineering Foundation, is now Systems Manager at the Daejeon Machinery Depot, Daejeon, Korea. R. M. GERMAN is Associate Professor, Materials Engineering Department, Rensselaer Polytechnic Institute, Troy, NY 12181.

Manuscript submitted April 15, 1983.

**Table I. Powder Characteristics**

| Parameter | Tungsten | Nickel | Iron |
|---|---|---|---|
| Vendor | GTE Products | Cotronics | Cerac |
| Purity, pct | 99.94 | 99.99 | 99.50 |
| Specific surface area, $m^2/g$ | 0.23 | 2.19 | 0.88 |
| Fisher subsieve size, $\mu m$ | 2.5 | 2.8 | 3.0 |
| Mean particle size, $\mu m$ | 2 to 3 | 3.3 | 10.8 |
| Apparent density, $g/cm^3$ | 2.65 | 2.15 | 2.41 |
| Major impurities (ppm) | Cr (5) | Ca (10) | Al (600) |
| | Fe (8) | Fe(30) | Ca (600) |
| | K (34) | Si (40) | Co (30) |
| | Mo (8) | | Cr (300) |
| | Na (7) | | Cu (300) |
| | Ni (6) | | Mn (2000) |
| | O (500) | | Ni (300) |
| | Si (10) | | Si (640) |
| | | | Ti (30) |

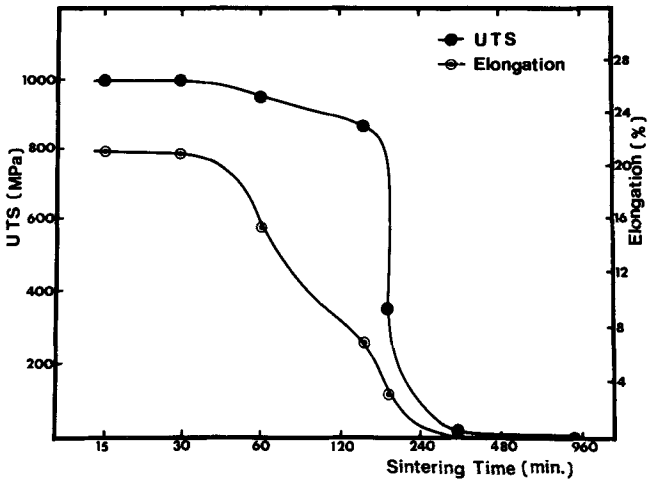


Fig. 1—The effect of sintering time on the strength and ductility. The composition is 95W-3.5Ni-1.5Fe, sintered at 1475 °C in dry hydrogen.

The sintered tensile bars were tested under uniaxial conditions in an Instron equipped with an extensometer. The gauge length was 20 mm. Additionally, bend tests were conducted to observe crack formation and propagation using a constant displacement fixture. This latter procedure allowed intermittent microstructural observations during crack propagation. Both optical and scanning electron microscopy have been applied to examine the fracture behavior.

## III. FRACTURE OBSERVATIONS

Sintered densities close to theoretical were achieved with sintering times as short as 15 minutes. Past research has shown densification is a prerequisite for adequate mechanical properties.[12,13,22] Furthermore, the cooling rate from the sintering temperature was sufficiently slow that solidification voids were avoided. Thus, the mechanical properties observed in this study are representative of the material. An example of the sintering time effect is given in Figure 1 for the 95W-3.5Ni-1.5Fe alloy sintered at 1475 °C. Strength shows little change for sintering times up to approximately two hours, but decreased with longer times. Ductility behaved very similarly. These observations agree with previous findings by Churn and Yoon.[13] It is expected that some property recovery is possible with prolonged sintering, on the order of 48 hours.[13]

The concern in this research has been with the fracture behavior associated with the changes represented in Figure 1. A comparison of fracture paths is given in Figure 2 for 95 and 93 pct W samples representing failure elongations of 15, 3, and 0 pct, respectively. Table II gives the results of quantitative analysis of the fracture modes. For this analysis, approximately 3 mm of fracture path was examined on each specimen. The results in Table II have an estimated ±5 pct variation. Four modes of crack extension are possible, tungsten cleavage, tungsten-grain boundary separation, matrix failure, and tungsten-matrix separation. Examination of Table II shows the proportion of tungsten cleavage increases with ductility. The amount of matrix failure also increases with specimen ductility. Similar results have been noted in prior studies.[6,12,13,23] The failure at the tungsten-tungsten grain boundaries occurs at low strains,

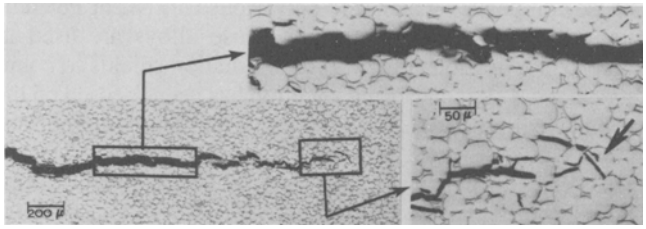

(*a*)

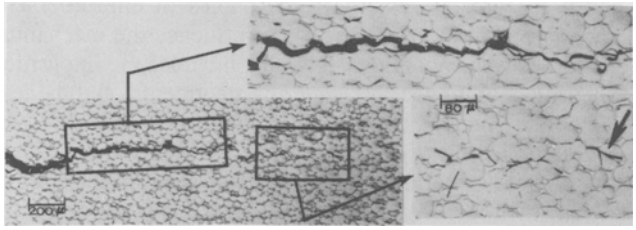

(*b*)

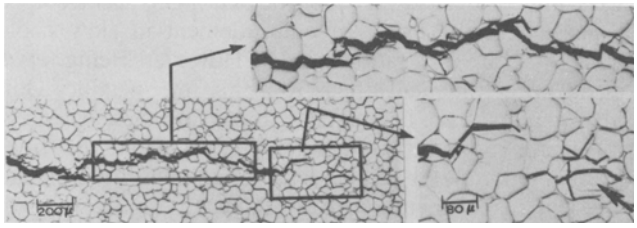

(*c*)

Fig. 2—Fracture paths in 93W-4.9Ni-2.1Fe sintered for 1.5 h (*a*), 95W-3.5Ni-1.5Fe sintered for 3 h (*b*), and 5.5 h (*c*). Properties for these alloys are listed in Table II.

these being weak.[6,15] Accordingly, the amount of failure at these boundaries will be dependent on the frequency of tungsten-tungsten contact, known as contiguity. Niemi *et al.*[24] have demonstrated the number of contracts per particle depends only on the volume fraction of liquid phase. Additionally, Stephenson and White[25] have shown that the size of the contacts in liquid phase sintered materials is

**Table II. Fracture Mode and Pct of Crack Path through the Tungsten, Matrix, *W*-Matrix, and *W*-*W* Boundary for the Fractures Shown in Figure 3**

| Composition | Sintering Temperature (°C) | Sintering Time (Hours) | Fracture Mode | Elongation (Pct) | Pct of Crack Path Through | | | |
|---|---|---|---|---|---|---|---|---|
| | | | | | *W* | Matrix | *W*-Matrix | *W*-*W* |
| 93W-4.9Ni-2.1Fe | 1465° ±5 °C | 1.5 | ductile | 15 | 68 | 8 | 2 | 22 |
| 95W-3.5Ni-1.5Fe | 1475° ±5 °C | 3 | brittle | 3 | 60 | 3 | 6 | 31 |
| 95W-3.5Ni-1.5Fe | 1475° ±5 °C | 5.5 | very brittle | 0 | 50 | 2 | 16 | 32 |

dependent on the grain size. Consequently, the proportion of tungsten-tungsten grain boundaries on the fracture surface depends only on the amount of tungsten. Failures at the tungsten-matrix interface and through the matrix were observed in all samples. The regions in front of the advancing crack tip exhibit both tungsten-tungsten boundary failure and transgranular cleavage. These cracks were created ahead of the crack before matrix phase rupture as seen in Figure 2.

Scanning electron microscopy further evidenced fracture behavior changes. Figure 3 shows fracture surfaces for the same specimens discussed above. The greater the ductility, the greater the proportion of tungsten cleavage and matrix phase failure. Also, decohesion of the tungsten-matrix interface is evident with low ductilities.

Figure 4 contrasts the microstructure of a 93W-4.9Ni-2.1Fe alloy at two regions during tensile testing. The alloy was sintered at 1465 °C for one hour, and then tensile-tested to 23.5 pct elongation. Necking was observed at the specimen center. Cracks have formed in the necked region and the tungsten grain shape is elongated. No cracking is observed away from the necked region and there is less tungsten grain elongation. Similar necking observations have been reported earlier by Churn and Yoon,[13] and Ekbom.[15] In Figure 5, the crack growth process is shown for this same alloy during continued elongation. Figure 5(a) corresponds to a 23.5 pct elongation while 5(b) corresponds to 24.5 pct. The cracks evident in (a) propagate at approximately a 45 deg angle with respect to the tensile axis. The crack formed at the lower strain [circled in (a), and (b)] opens with straining and propagates into the neighboring microstructure. This evidence suggests that a change in fracture path occurs during failure. Tungsten cleavage cracks form at low strains. These initial cracks change direction by about 45 deg at the neighboring interface. Propagation continues along directions of maximum stress, possibly changing direction at interfaces as shown schematically in Figure 6. Examination of Figure 5 shows that the circled crack preferentially extended during deformation. The other cracks appeared to be stable in size. Such evidence suggests that several cracks initiate early during deformation. However, only a few cracks actually undergo extension with subsequent stressing; thus, the failure is probably governed by crack propagation and not initiation. Also, failure is dominated by crack growth through the matrix and not by linkage of the initial small cracks.

## IV. DUCTILITY DEPENDENCE ON THE CONTIGUITY

Several investigations of heavy alloys have provided evidence of a microstructural dependence for the ductility. During tensile deformation, the hard tungsten grain surrounded by the softer matrix phase is submitted to a hydrostatic

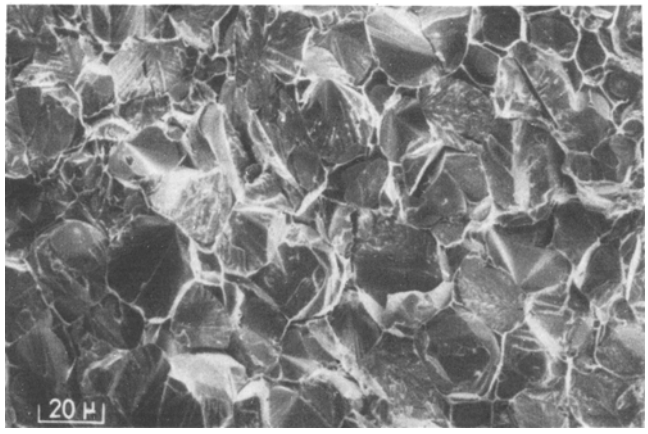


(*a*)

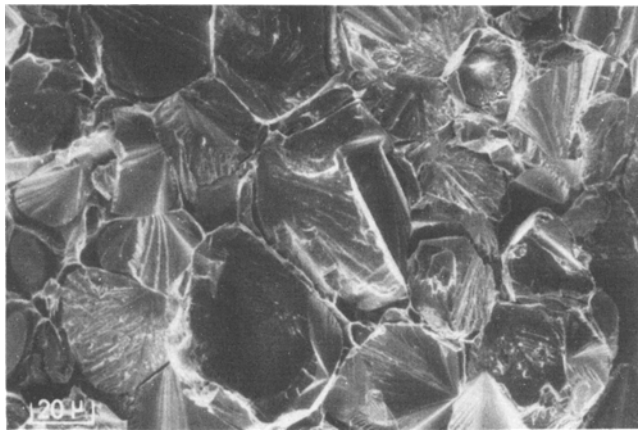


(*b*)

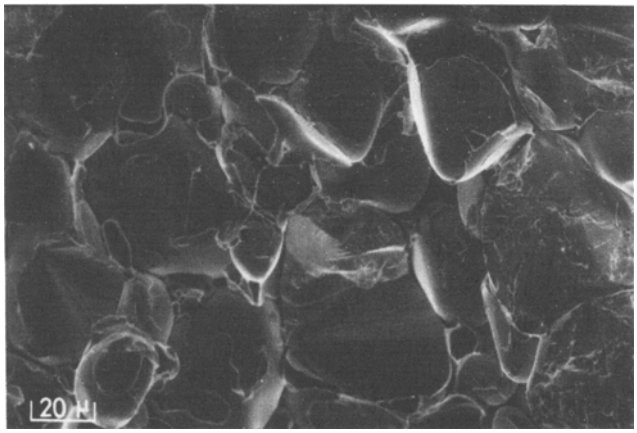


(*c*)

Fig. 3—Scanning electron micrographs of the fracture surfaces of 93W-3.9Ni-2.1Fe sintered for 1.5 h (*a*), 95W-3.5Ni-1.5Fe sintered for 3 h (*b*), and 5.5 h (*c*) [corresponding to Fig. 2 and Table II].

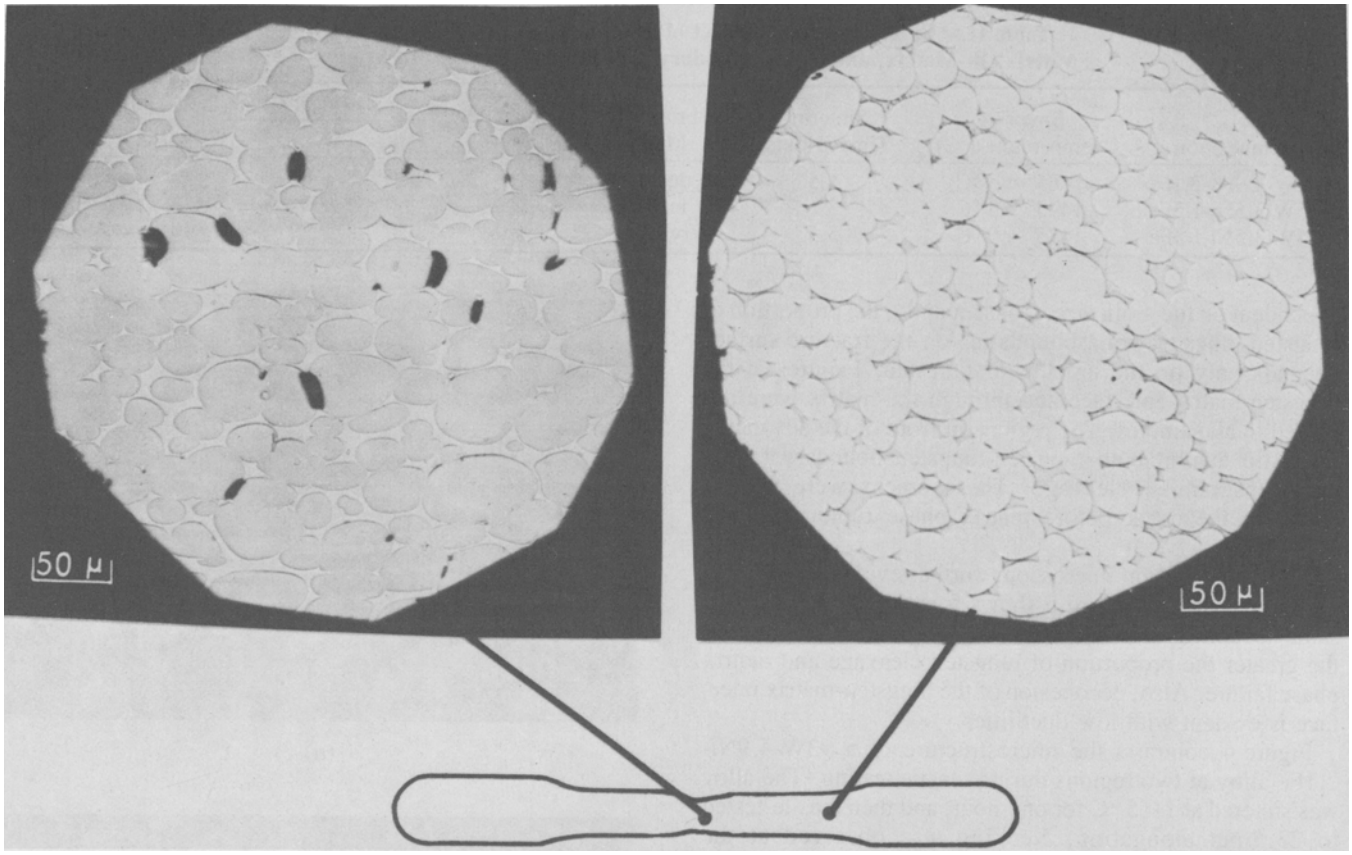


Fig. 4—The microstructure of a tensile specimen with the composition of 93W-4.9Ni-2.1Fe, sintered for 1 h and pulled to a 23.5 pct elongation at room temperature.

stress such as shown in Figure 7. As the tungsten content increases, there is less chance for the tungsten grain to be completely surrounded by matrix phase.[24] Accordingly, there is a higher tungsten contiguity as the volume fraction of solid increases. The amount of tungsten-tungsten contact is expressed as the contiguity $C_w$, defined as,

$$C_w = \frac{S_{w-w}}{S_w} \quad [1]$$

where $S_w$ is the surface area of tungsten grains and $S_{w-w}$ is the surface area involved in tungsten-tungsten contacts. In Figure 8, the maximum shear stress on a tungsten grain $\tau_{max}$ is expressed as

$$\tau_{max} = \frac{\sigma_T + \sigma_C}{2} \quad [2]$$

where $\sigma_T$ and $\sigma_C$ are the tensile and compressive components, respectively. The tensile component $\sigma_T$ is due to the applied tensile stress. Contact between the tungsten grains will alter the compressive stress as follows:

$$\sigma'_C = \sigma_C \frac{S_{w-m}}{S_w} = \sigma_C(1 - C_w) \quad [3]$$

where $\sigma'_C$ is the new compressive component, reflecting the diminished matrix-tungsten interface area as measured by $S_{w-w}$, where

$$\frac{S_{w-m}}{S_w} + \frac{S_{w-w}}{S_w} = 1$$

Assuming the compressive stress $\sigma_C$ is proportional to the applied tensile stress $\sigma_T$, leads to

$$\sigma'_C = k\sigma_T(1 - C_w) \quad [4]$$

with $k$ being the proportionality factor. A combination of Eqs. [2] and [4] gives

$$\tau_{max} = (\sigma_T/2)[1 + k(1 - C_w)] \quad [5]$$

The basic stress-strain behavior for heavy alloys follows the form[14]

$$\tau = \tau_0 \varepsilon^m \quad [6]$$

where $\tau_0$ and $m$ are material constants, and $\varepsilon$ is the strain. Equation [5] applies to the microscopic W grain while Eq. [6] applies to the composite heavy metal system. We assume that the maximum shear stress yield criterion of Eq. [5] reaches the level of $\tau$ in Eq. [6] when the tungsten particles begin to elongate.[14,16,26] From a combination of Eqs. [5] and [6],

$$\varepsilon^m = \frac{\sigma_T}{2\tau_0}[1 + k(1 - C_w)] \quad [7]$$

For this analysis, it is assumed that tensile failure occurs when the stress $\sigma_T$ approaches a critical failure level $\sigma_f$; thus, a general relation between the strain to failure and the contiguity will appear as,

$$\varepsilon_f^m = K_1 + K_2(1 - C_w) \quad [8]$$

with $K_1$ and $K_2$ representing a collection of material constants and $\varepsilon_f$ equal to the failure strain (elongation).

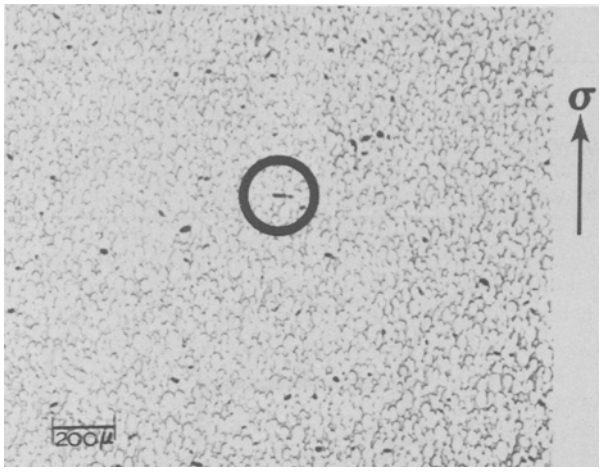


(*a*)

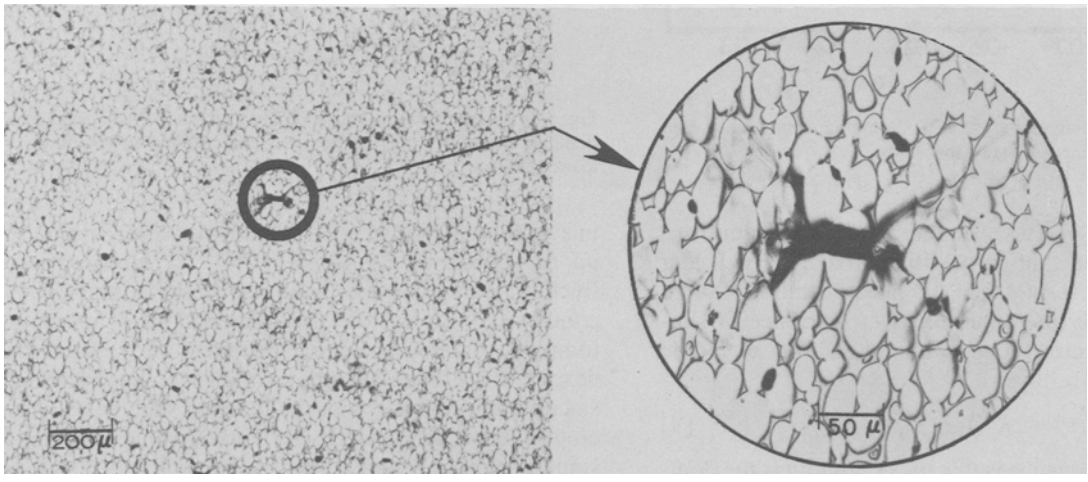


(*b*)

Fig. 5 — The microstructures of the neck region at elongations of 23.5 pct (*a*) and 24.5 pct (*b*) in the 93W-4.9Ni-2.1Fe specimen sintered for 1 h.

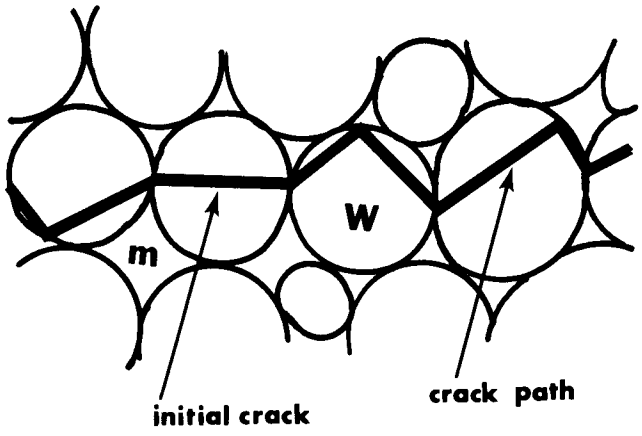


Fig. 6 — Illustration of the fracture mode and the changing crack path at interfaces.

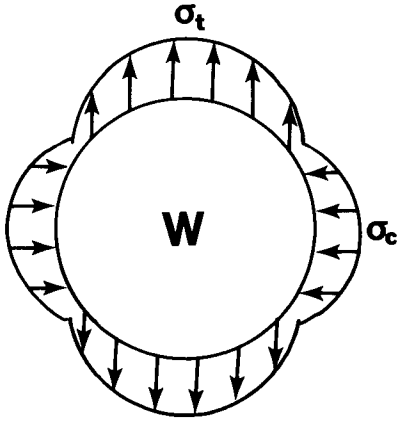


Fig. 7 — Schematic representation of stresses around a tungsten grain from the matrix during tensile testing.

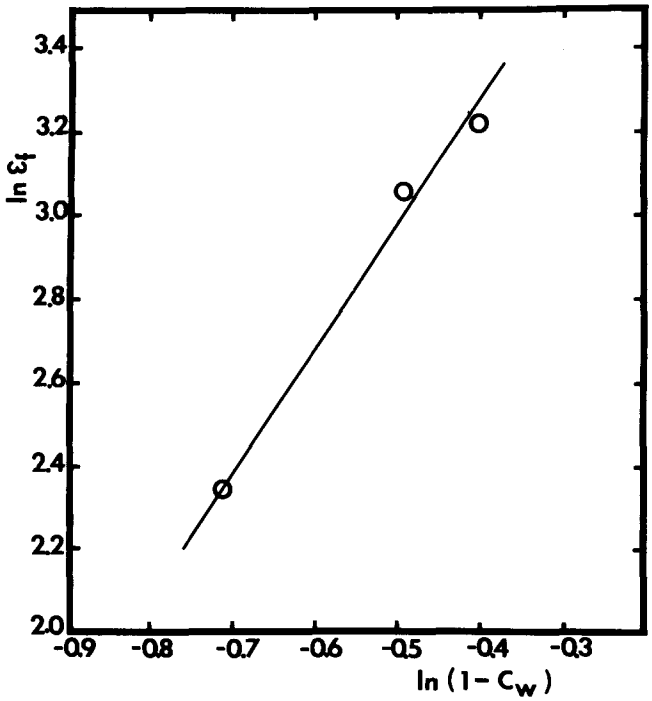


Fig. 8 — A plot of the contiguity effect ($C_W$) on the maximum elongation for the 3 heavy metal compositions of this study.

**Table III. Maximum Elongation and Contiguity with Different Composition**

| Composition | Sintering Temp. (°C) | Sintering Time (Hr.) | Max. Elong. | Contiguity |
|---|---|---|---|---|
| 93W-4.9Ni-2.1Fe | 1465° ±5 | 1 | 25.0 | 0.33 |
| 95W-3.5Ni-1.5Fe | 1475° ±5 | 0.25 | 21.6 | 0.39 |
| 97W-2.1Ni-0.9Fe | 1485° ±5 | 0.25 | 10.4 | 0.51 |

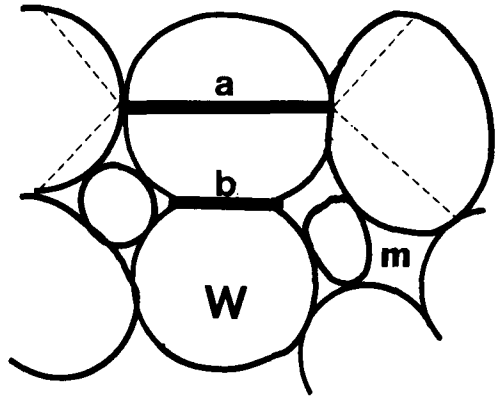


Fig. 9 — A schematic illustration of a transgranular crack (*a*) and an intergranular crack (*b*) and the possible compression of the latter by the matrix phase.

In heavy alloy systems, as the tungsten content approaches 100 pct, the contiguity will approach unity. Under the condition of $C_w = 1.0$, then the plastic strain to failure is zero, consequently the value of $K_1 \approx 0$. Hence, a simplified model for microstructural limited ductility would be as follows for heavy alloys:

$$\varepsilon_f^m = K_2(1 - C_w) \qquad [9]$$

The important consequence is that the contiguity is the dominant factor in promoting high ductilities. Table III gives the maximum elongation and contiguity for the three heavy alloy compositions of this study. These data are plotted according to the form of Eq. [9] in Figure 8. The slope of this plot corresponds to $1/m$ and has a value of 1.4, giving $m = 0.7$.

## V. DISCUSSION

It has been observed in earlier studies that cracks form preferentially at the tungsten-tungsten grain boundaries.[6,13–15] Also, transgranular cracking occurs before failure as demonstrated in Figure 5. The transgranular cracks are larger than the intergranular cracks as illustrated in Figure 9. The stress concentration necessary for transgranular failure is higher than that for intergranular failure. The matrix phase plays an important role in hindering crack propagation.

In some respects, the fracture observations on tungsten heavy alloys resemble earlier findings on cemented carbides. A major difference is in the ductility, while there are similarities with respect to sensitivity to interfacial contamination, porosity, composition, amount of matrix phase, and microstructure.[27–40] The exact interaction of these parameters with respect to fracture of cemented carbides is still unresolved. The transverse rupture strength (brittle failure) increases with the mean free path between carbide grains up to approximately 0.5 $\mu$m.[27,30–34,39] Furthermore, the fracture strength varies with the carbide grain size and contiguity.[32–36] Various refinements have attempted to lump these microstructural features into composite indexes.[27,30,33,34] Such an approach is generally unsatisfactory since failure initiates with the defects, such as residual microporosity.[38] In general, the crack propagation mode is similar between heavy alloys and cemented carbides. However, the differences in crack initiation and deformation of the hard phase are significant. Thus, the difference in inherent ductility leads to a focus on the tungsten-matrix interface and its role in affecting plastic deformation of the tungsten grains. Such a concern in the cemented carbides shows the crack resistance decreases linearly with an increasing contiguity.[27] This contrasts with the current findings for heavy metal ductility dependence on contiguity as given in Eq. [9].

Previous studies have suggested ductile fracture evidences a high degree of transgranular cleavage of tungsten grains.[6,13] A brittle heavy alloy tends to show more matrix-tungsten separation. Such observations are often correlated to improper processing; these concerns go beyond the composition and microstructure effects treated here. For a fixed contiguity, the ductility depends on the tungsten-matrix interfacial properties. Alternatively, for a fixed interface condition the ductility will vary with the microstructure, specifically the contiguity. In this study, the fracture path has been observed and quantitatively analyzed *vs* the ductility (Table II). The results show the binding energy between the tungsten and matrix phase is a key determinant of ductility. The greater this binding energy, the greater the ductility. Several factors can degrade the strength of the tungsten-matrix binding energy and thereby embrittle heavy alloys. This includes impurity segregation,[6,7,23,26,41]

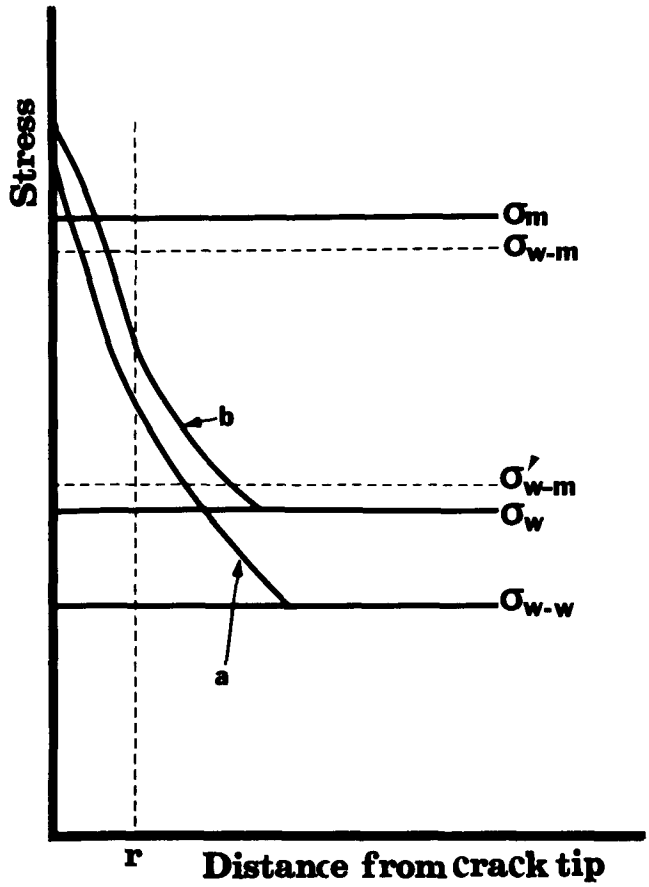


Fig. 10— An illustration of stress concentration curves by an intergranular crack (*a*) and a transgranular crack (*b*), and of a fracture mode dependence on the *W*-matrix interfacial strength, $\sigma_{w\text{-}m}$ and $\sigma'_{w\text{-}m}$.

intermetallic formation,[1,2,18,19,42] porosity,[12,13,42] adsorbed hydrogen,[9–11,43] and chemical segregations.[21,44] The tungsten-tungsten binding energy is quite low, hence failure is observed at low strains.[45,46] The propagation of either a transgranular or intergranular crack will be along the weakest path. If the tungsten-matrix binding energy is sufficiently high, crack propagation will be retarded by the presence of the matrix. The advancing crack will have a stress concentration in front of itself. If the contiguity is low, the tungsten-matrix binding energy is high, and the mean free path between tungsten grains high, then the matrix phase will hinder crack propagation. On the other hand, if the tungsten-matrix interface is weak, then the stress concentration will exceed this strength and propagation of the crack will occur along the interface. In this latter case, the relative amount of transgranular failure will depend on the crack orientation and the relative matrix-tungsten interfacial energy. Figure 10 illustrates how such a concept of relative interfacial energies can be used to explain the fracture path differences. Under an increasing applied stress, failure will occur first at the tungsten-tungsten interface. With the concomitant increase in stress intensity (crack tip effect) as well as increased loading, the stress concentration next reaches a level capable of failure by tungsten cleavage. The cracks that have formed build the stress concentration profiles "a" or "b" corresponding to either an intergranular or transgranular source. At a distance *r* from these cracks, the relative energy of the tungsten-matrix (*w-m*) interface becomes important. If this energy is sufficiently high, crack propagation will be hindered by the matrix. Alternatively, if the interfacial energy is low corresponding to $\sigma'_{w\text{-}m}$, the crack will continue to propagate along the tungsten-matrix interface. Consequently, the tungsten-matrix interfacial energy is the dominant concern with respect to large elongations.

Past research has shown several processing factors contribute to the tungsten-matrix interfacial energy.[1–23,41–44] Our analysis has not specifically addressed these various factors. However, it is demonstrated that the cohesive energy of the tungsten-matrix interface is a major factor in determining the ductility of heavy metal alloys. The concept discussed above suggests that future efforts to improve the tensile behavior should focus on the tungsten-matrix interfacial energy. If the tungsten-matrix interfacial energy is sufficiently high, the contiguity is the major determinant of ductility in heavy alloys. This fact is shown by Eq. [9] and the data given in Figure 8.

## VI. CONCLUSION

Initial cracks form not only between the tungsten-tungsten boundaries, but also in the tungsten grain during tensile testing. The transgranular cracks are more favorable to continual propagation because of their size and the surroundings.

The ductility of the heavy alloys is governed by the binding energy between the tungsten-matrix phase. The weaker this binding energy the lower the ductility to failure.

In heavy alloys, the maximum elongation depends strongly upon its contiguity. A high contiguity produces a lower ductility.

Future efforts aimed at improving the properties of liquid phase sintered heavy alloys should address the tungsten-matrix interface binding energy.

## ACKNOWLEDGMENT

The authors wish to thank Norman Gendron of R.P.I. for his aid with the optical microscopy. Partial support for this research was provided by the Lawrence Livermore National Laboratory.

## REFERENCES

1. D. V. Edmonds and P. N. Jones: *Metall. Trans. A*, 1979, vol. 10A, pp. 289-95.
2. R. V. Minakova, A. N. Pilyankevich, O. K. Teodorovich, and I. N. Frantsevich: *Soviet Powder Met. Metal Ceram.*, 1968, vol. 7, pp. 396-99.
3. R. V. Minakova, A. N. Pilyankevich, O. K. Teodorovich, and I. N. Frantsevich: *Soviet Powder Met. Metal Ceram.*, 1968, vol. 7, pp. 473-77.
4. E.-T. Henig, H. Hofmann, and G. Petzow: *Proceedings of the 10th Plansee-Seminar*, H. M. Ortner, ed., Metallwerk Plansee, Reutte, Austria, 1981, vol. 2, pp. 335-59.
5. D. J. Jones and P. Munnery: *Powder Met.*, 1967, vol. 10, pp. 156-73.
6. R. M. German and J. E. Hanafee: *Processing of Metal and Ceramic Powders*, R. M. German and K. W. Lay, eds., TMS-AIME, Warrendale, PA, 1982, pp. 267-82.
7. B. C. Muddle and D. V. Edmonds: *Phil. Trans. Royal Soc. Lond.*, 1980, vol. A295, p. 129.
8. L. G. Bazhenova, A. D. Vasilev, R. V. Minakova, and V. I. Trefilov: *Soviet Powder Met. Metal Ceram.*, 1980, vol. 19, pp. 34-38.
9. H. K. Yoon, S. H. Lee, S-J. L. Kang, and D. N. Yoon: *J. Mater. Sci.*, 1983, vol. 18, pp. 1374-80.

10. C-C. Ge, X-I. Xia, and E-T. Henig: *Proceedings P/M-82* (International Powder Metallurgy Conference, Florence, Italy, June 1982), *Associazione Italiana di Metallurgia*, Milano, Italy, 1982, pp. 709-14.
11. M. Yodogawa: *Sintering-Theory and Practice*, D. Kolar, S. Pejovnik, and M. M. Ristic, eds., Elsevier Scientific Pub. Co., Amsterdam, Netherlands, 1982, pp. 519-25.
12. T. K. Kang, E-T. Henig, W.A. Kaysser, and G. Petzow: *Modern Developments in Powder Metallurgy*, H. H. Hausner, H. W. Antes, and G. D. Smith, eds., Metal Powder Industries, Princeton, NJ, 1981, vol. 14, pp. 189-203.
13. K-S. Churn and D. N. Yoon: *Powder Met.*, 1979, vol. 22, pp. 175-78.
14. R. H. Krock and L. A. Shepard: *Trans. TMS-AIME*, 1963, vol. 227, pp. 1127-34.
15. L. Ekbom: *Modern Developments in Powder Metallurgy*, H. H. Hausner, H. W. Antes, and G. D. Smith, eds., Metal Powder Industries Federation, Princeton, NJ, 1981, vol. 14, pp. 177-88.
16. R. H. Krock: *Metals for the Space Age*, F. Benesovsky, ed., Metallwerk Plansee, Reutte, Austria, 1965, pp. 256-75.
17. R. H. Krock: *J. Materials*, 1966, vol. 1, pp. 278-92.
18. J. F. Kuzmik: *Modern Developments in Powder Mettallurgy*, H. H. Hausner, ed., Plenum Press, New York, NY, 1966, vol. 3, pp. 166-72.
19. H. Takeuchi: *Nippon Kinzoku Gakkaishi*, 1967, vol. 31, pp. 1064-69.
20. E. G. Zukas: *Metall. Trans. B*, 1976, vol. 7B, pp. 49-54.
21. I. Y. Kzykovich, R. V. Makarova, O. K. Teodorovich, and I. N. Frantsevich: *Soviet Powder Met. Metal Ceram.*, 1965, vol. 4, pp. 655-60.
22. J. M. Googin, W. L. Harper, A. C. Neeley, and L. R. Phillips: "Development of Ductile Tungsten Alloys," Report Y-1364, Y-12 Plant, Union Carbide Nuclear Division, Oak Ridge, TN, August 1961.
23. M. R. Eisenmann and R. M. German: *Prog. Powder Met.*, 1982, vol. 38, pp. 203-13.
24. A. N. Niemi, L. E. Baxa, J. K. Lee, and T. H. Courtney: *Modern Developments in Powder Metallurgy*, H. H. Hausner, H. W. Hausner, H. W. Antes, and G. D. Smith, eds., Metal Powder Industries Federation, Princeton, NJ, 1981, vol. 12, pp. 483-95.
25. I. M. Stephenson and J. White: *Trans. Brit. Ceramic Soc.*, 1967, pp. 443-83.
26. L. Ebkom: *Scand. J. Metallurgy*, 1976, vol. 5, pp. 179-84.
27. G. Grathwohl and R. Warren: *Mater. Sci. Eng.*, 1974, vol. 14, pp. 55-65.
28. M. Komac and L. Lange: *Inter. J. Powder Met. Powder Tech.*, 1982, vol. 18, pp. 313-21.
29. K. S. Cherniavsky: *Sci. Sintering*, 1982, vol. 14, pp. 1-12.
30. J. R. Pickens and J. Gurland: *Mater. Sci. Eng.*, 1978, vol. 33, pp. 135-42.
31. J. Gurland and P. B. Bardzil: *Trans. AIME*, 1955, vol. 203, pp. 311-15.
32. J. Gurland: *Trans. TMS-AIME*, 1963, vol. 227, pp. 1146-50.
33. J. L. Chermant and F. Osterstock: *Powder Met. Inter.*, 1979, vol. 11, pp. 106-09.
34. J. L. Chermant and F. Osterstock: *J. Mater. Sci.*, 1976, vol. 11, pp. 1939-51.
35. R. Warren and M. B. Waldron: *Powder Met.*, 1972, vol. 15, pp. 166-80.
36. H. C. Lee: Ph. D. Thesis, Brown University, 1977.
37. H. Suzuki and K. Hayashi: *Trans. Japan Inst. Metals*, 1969, vol. 10, pp. 360-64.
38. P. B. Anderson: *Panseeber. Pulverment.*, 1967, vol. 15, pp. 180-86.
39. F. V. Lenel: *Powder Metallurgy Principles and Applications*, Metal Powder Industries Federation, Princeton, NJ, 1980, pp. 383-400.
40. H. E. Exner and J. Gurland: *Powder Met.*, 1970, vol. 13, pp. 13-30.
41. C. Lea, B. C. Muddle, and D. V. Edmonds: *Metall. Trans. A*, 1983, vol. 14A, pp. 667-77.
42. H. H. Hausner: *Metals and Alloys*, 1943, vol. 18, pp. 437-40.
43. F. E. Sczerzenie and H. Rogers: *Hydrogen in Metals*, I. M. Bernstein and A. W. Thompson, eds., ASM, Metals Park, OH, 1974, pp. 645-55.
44. V. G. Bukatov, V. M. Romashov, and Y. V. Gostev: *Soviet Powder Met. Metal Ceram.*, 1982, vol. 21, pp. 785-88.
45. A. Joshi and D. F. Stein: *Metall. Trans.*, 1970, vol. 1, pp. 2543-46.
46. J. R. Stephens: *High Temperature Materials II*, G. M. Ault, W. F. Barclay, and H. P. Munger, eds., Interscience Publ., New York, NY, 1963, pp. 125-37.